

A Cost-Effective Solution for Measuring Vibration and Impact on Small Twin Engine Electric Fixed Wing UAV

Yusuf Giri Wijaya

Research Center for Aeronautics Technology, National Research and Innovation Agency

Fuad Surastyo Pranoto

Research Center for Aeronautics Technology, National Research and Innovation Agency

Rizaldi, Ardian

Research Center for Aeronautics Technology, National Research and Innovation Agency

Nurrohmad, Abian

Research Center for Aeronautics Technology, National Research and Innovation Agency

他

<https://doi.org/10.5109/7236880>

出版情報 : Evergreen. 11 (3), pp.2367-2385, 2024-09. 九州大学グリーンテクノロジー研究教育センター

バージョン :

権利関係 : Creative Commons Attribution 4.0 International

A Cost-Effective Solution for Measuring Vibration and Impact on Small Twin Engine Electric Fixed Wing UAV

Yusuf Giri Wijaya^{1,2,*}, Fuad Surastyo Pranoto¹, Ardian Rizaldi^{1,3},
Abian Nurrohmad¹, Prasetyo Ardi Probo Suseno¹, Angga Septiyana¹,
Gunawan Setyo Prabowo¹, Aditya Rio Prabowo^{4,*}

¹Research Center for Aeronautics Technology, National Research and Innovation Agency, Bogor, Indonesia

²Magister Program of Instrumentation and Control, Faculty of Industrial Technology,
Institut Teknologi Bandung, Bandung, Indonesia

³Graduate School of Mechanical and Aerospace Engineering, Gyeongsang National University, Jinju 52828,
Republic of Korea

⁴Department of Mechanical Engineering, Universitas Sebelas Maret, Surakarta, Indonesia

* Author to whom correspondence should be addressed:

E-mail: yusuf.giri.wijaya@brin.go.id (Y.G.W.), aditya@ft.uns.ac.id (A.R.P.)

(Received October 28, 2023; Revised June 23, 2024; Accepted September 7, 2024).

Abstract: Unmanned Aerial Vehicles (UAVs) have gained widespread popularity in various fields, leading to a demand for reliable and cost-effective measurement systems to ensure the safe and efficient operation of these UAVs. One of the vital aspects to ensure the UAV safe operation is the vibration information that occurs during the flight to detect anomalies that may be caused by failures or other factors. At the operational aspect, the vibration data that recorded during the flight test can be used to design the damper system to minimize the vibration effect during the aerial photography mission. This research proposes a low-cost vibration and impact measurement system for small electric fixed-wing UAVs. The system utilizes accelerometers to measure the vibration and impact levels experienced by the aircraft during flight. We designed and tested the system on a small electric fixed-wing UAV and compared its results with a commercial measurement system. This allows us to evaluate the accuracy and reliability. The experimental results demonstrated that our system can accurately measure the vibration and impact levels experienced by small electric fixed-wing UAVs during flight. Furthermore, our system was found to be reliable and cost-effective compared to the commercial measurement system with differences in vibration measurement in the range of 10% with some parameters even below 6%, impact measurement in the range of 2-4%, and the total cost amounts of the component is USD 62.84. This research provides a low-cost solution for monitoring vibration and impact levels of small electric fixed-wing UAVs.

Keywords: Measurement System; Vibration; Impact; cost-effective; UAV

1. Introduction

Unmanned Aerial Vehicles (UAVs) have gained significant attention in recent years due to their ability to perform a wide range of tasks in various fields, including surveillance, mapping, inspection, and delivery. With the increasing demand for UAVs, there is a need for reliable and cost-effective measurement systems to ensure the safe and efficient operation of these aircraft.

One important aspect of UAV operation is monitoring the vibration and impact levels experienced during flight. Vibration phenomena in unmanned aircraft may originate from aerodynamic forces, engine vibrations, control surface deflection, and system malfunctions. Vibrations

can also be generated from environmental causes such as gusts of wind and turbulence. Subsystems in UAVs such as MEMS gyros, cameras, and accelerometers can become sensitive to vibration, and filtration algorithms cannot always solve this problem^{1,2}). Vibration is also a major cause of structural failure due to fatigue. In addition, vibration can affect the aerodynamic behavior of the aircraft³). Excessive vibration can also interfere with the mission undertaken⁴). For example, an aircraft with a photography mission that experiences excessive vibration will be greatly disturbed and cause the photography results to be not optimal. The vibration profiles recorded during the flight test are very useful for designing the damper system for the camera, as we know that the

vibration can influence the camera performance in a bad direction, preventing it from producing a crisp and clear image during the aerial photography mission.

Therefore, there is a need for a low-cost, reliable, and accurate vibration and impact measurement system for small electric fixed-wing UAVs. In this research, we aim to design and test a low-cost system that can accurately measure the vibration and impact levels experienced by small electric fixed-wing UAVs during flight. Accelerometers are used in the proposed system to measure the impact and vibration levels.

An accelerometer is a device that measures the vibration, or acceleration of motion, of a structure. The force caused by vibration or a change in motion (acceleration) causes the mass to “squeeze” the piezoelectric material which produces an electrical charge that is proportional to the force exerted upon it. Since the charge is proportional to the force, and the mass is constant, then the charge is also proportional to the acceleration, therefore it can be used to measure the vibration and impact.

Utilizing a small electric fixed-wing UAV, we will carry out experiments and compare our system's results with those of a calibrated measurement device in ground before conducting the flight test. We will be able to evaluate the accuracy of our system thanks to this comparison. The expected maximum frequency range of the vibration during the UAV operation will come from engine and propeller rotation which equal to 100 Hz. Thus, we use 1000 Hz sampling rate to capture this data.

Several vibration studies on UAV systems have been carried out previously. Kumar and Devendra presented an experimental study that focused on measuring UAV container vibrations using high-order moments to demonstrate the nature of vibrations in containers as non-stationary and non-gaussian⁵⁾. Radkowski and Szulim presented a solution to the vibration problem that arises in quad-copter maneuvers. The main source of vibration on their approach comes from the unbalance of the motor and/or propeller⁶⁾. Fresk and Nikolakopoulos established an induced skeletal vibration and attenuation scheme⁷⁾. They discussed vibrations in UAVs and modeled them as a sinusoidal angular vibration and a random angular vibration. Cai et al. Discusses the main vibration sources in helicopter UAVs. The three main sources are the rotation of the main motor, tail motor, and engine. They estimated the frequency of these three parts based on a motor speed of 1850 rpm⁸⁾. Dunbabin et al. mention that UAV systems produce a unique and challenging environment in which all systems must operate properly⁹⁾. Plasencia et al modeled the UAV system, generated a range of vibrations originating from the main rotor and designed a control methodology based on an adaptive neuro-fuzzy inference system to dampen unwanted

vibrations¹⁰⁾. Luber and Becker have conducted experimental vibration investigations on aircraft and they able to predict the aircraft vibration by measuring the unsteady pressures on wind tunnel models using polvinylidenfluorid (PVDF) sensor¹¹⁾.

On manned aircraft, vibrations can be felt by the flight crew and may be detected through sight and sound. In UAVs, vibrations can only be detected from instruments dedicated to measuring vibrations. The shape of the vibration on the small UAV resembles sinusoidal motion¹²⁾. Vibration in the UAV is a complex matter that is affected by the actuation unit and aerodynamic forces¹³⁾. Since the inertial measuring device is mounted directly on the UAV, it is sensitive to nature or random vibration of the vehicle¹⁴⁾. Vibration on the aircraft can be predicted through statistical approaches such as the Generalized Likelihood Ratio Test (GLRT)¹⁵⁾ or through the Particle Swarm Optimization (PSO)¹⁶⁾ and Support Vector Machine (SVM)¹⁶⁾ methods.

Impact measurement is also a vital aspect of UAV development, as it provides critical information about the mechanical load that the UAV components experience during operation¹⁷⁾. These loads can cause failure of critical components, leading to catastrophic consequences. Therefore, it is essential to measure the impact loads on UAVs accurately and efficiently to ensure their safe and reliable operation¹⁸⁾. Existing solutions for measuring impact loads on UAVs are often complex and expensive, limiting their practical applications. Furthermore, many of these solutions require additional equipment or modifications to the UAV, which can affect its weight, balance, and aerodynamics.

This paper presents a novel solution for measuring vibration and impact loads on UAVs. The proposed solution is simple, lightweight, and cost-effective, making it suitable for an electric twin-engine fixed-wing UAV. The experimental study involves both ground tests and flight tests to validate the proposed solution and assess its performance in real-world scenarios. The ground test involves vibration and impact tests, while the flight test involves monitoring the UAV's behavior during flight. The results of the experimental study demonstrate the effectiveness and reliability of the proposed solution in measuring vibration and impact loads on UAVs.

2. Methodology and Design Requirements

The methodology is a set of stages executed by a researcher to produce the prototype that has functionality as defined. In this paper, the developed prototype is a measurement system that can fit into the small UAV/Drone, measuring the vibration during flight and the impact load at landing. The research methodology consists of several steps, as shown in Fig. 1

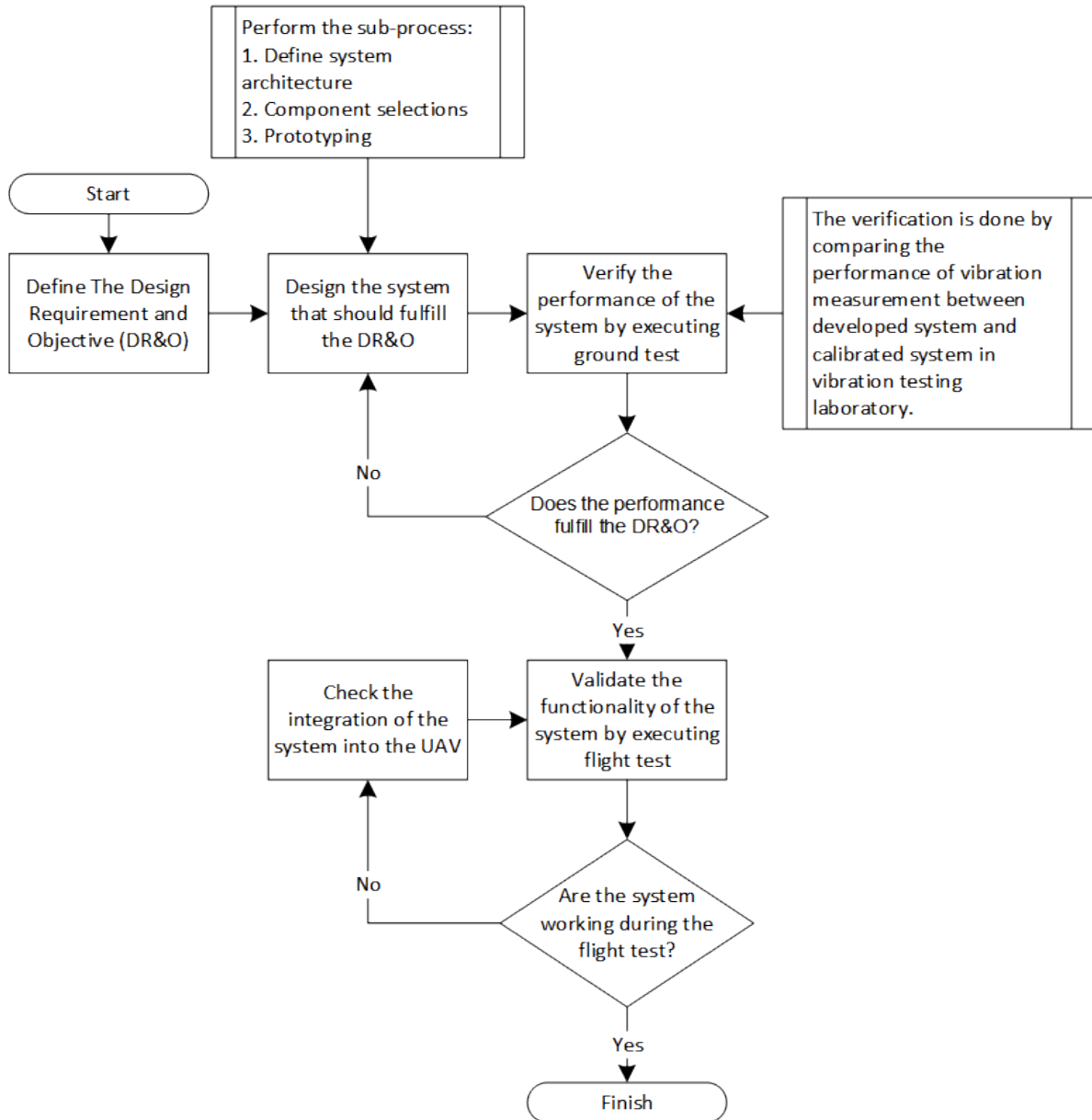


Fig. 1: Flowchart of Research Methodology

The first step defined the design requirement and objective of the measurement system. For the objective, the system will measure and record the vibration on the UAV during the flight. In addition, the system also has the capability to measure and record the impact load during the landing phase. This capability is required by the structural engineer to ensure the value of impact load during landing is not exceeding the airframe structural limit.

The requirements are derived from these objectives. There are two requirement categories: requirements related to the functionality and performance of the system.

The functional requirement covers all aspects that have an influence on the functionality of the system, while the performance requirement covers all aspects related to how well the system will measure and record the parameters related to the vibration and impact load. The performance requirement will be measured by comparing the measurement result of the experimental system with the calibrated system at the vibration laboratory. The functional requirement can be seen in Table 1, while the performance requirement is in Table 2.

Table 1. Functional Requirement

No	Aspect	Requirement	Compliance Criteria
I.1	Dimension and weight of the system	<p>The system, including the microcontroller for data acquisition, sensors, power supply, should fit into the cabin of the UAV for the test bench and the weight should not exceed the UAV capability.</p> <p>The dimension of the system should not exceed the following: 28cm x 16 cm x 11 cm.</p> <p>The weight of the system, including the power supply should not exceed 500 grams.</p>	<p>Install the whole system into the UAV. Inspect and check visually to ensure the whole system is installed and functioning normally.</p> <p>Before the installation, the weight of the whole system should be measured.</p>
I.2	Power supply	<p>The system should be powered by DC (direct current) power with the voltage range of 9 to 12 V. The electrical power shall be independent, not dependent on the UAV main power supply. The separation of the power supply from the UAV main power supply is necessary to not disturb the main UAV power supply which can lead to catastrophic consequences. The operational time requirement at least 60 minutes.</p>	<p>Inspect the power supply rating visually and check if the rating meets with the requirement or not. Connect the power supply to the system and check whether the system is turning on and functioning properly or not.</p>
I.3	Vibration and impact Measurement	<p>In order to measure the vibration and impact load, the system should have the following components: The microcontroller and the sensor.</p> <p>The microcontroller should have a built in micro-SD card reader. The micro-SD card reader will enable the recording functionality directly on the microcontroller board without sacrificing the compactness of the system. In order to ensure the high performance of measurement during the high sampling rate measurement scenario, the higher clock microcontroller is preferable.</p> <p>The sensor for measuring the vibration is an accelerometer. The accelerometer should be able to measure the accelerations in the X, Y, and Z-axis that occur between the frequency ranges of 0 – 400 Hz with the sampling rate of 1024 Hz.</p> <p>The impact load measurement should use the same sensor as the vibration measurement to ensure the compactness of the system. The sensor should be able to measure the impact load up to 16g.</p> <p>The system should use a minimum of 1 sensor for measuring the acceleration in X, Y, and Z-axis.</p>	<p>Inspect the datasheet of the components. Select the component not only based on the fulfillment of the requirement but also the price and size limitations.</p> <p>The actual performance of vibration and impact measurement of the developed system will be tested in the vibration laboratory.</p>
I.4	Recording function	<p>The system should be able to not only measure the vibration and impact load during the flight but also record the result into the micro-SD card. The recorded result should be written in .txt format and save the acceleration on each axis with a coma-separated value.</p>	<p>The recording function will be tested in the vibration laboratory.</p>
I.5	Cost to built	<p>In order to keep the system cost-effective, the cost to build the system should not exceed \$100. The price to build the system should be cheaper than the UAV price where this system will be installed. For the purposes of the test, the system will be installed on the foam based small UAV, with the MTOW of 12 kg.</p> <p>The cost should cover all materials to build this system, including the microcontroller, the sensor, the power supply, and other peripherals.</p>	<p>Identify the price for each material for building this system and sum all to get the total price. However, the man-hours cost to build the system is excluded from the total cost.</p>

The sensor we used for measuring the vibration is an accelerometer. This accelerometer able to measure the accelerations in the X, Y, and Z-axis that occur between the frequency ranges of 0 – 400 Hz with the sampling rate of 1024 Hz. The maximum frequency range is calculated from the maximum rotation of the electric motor used by the UAV which is 5500 rpm and equivalent to the 92 Hz. The frequency range of the impact is well between the frequency range for vibration.

As stated earlier in this chapter, UAV-based aerial mapping normally uses the camera to capture the image. However, the camera is attached to the UAV airframe during the flight, it is prone to the vibrations that are generated by the UAV engines and other external factors, like gust or turbulence. When the camera vibrates, it will reduce the ability to produce clear and crisp images and make the image unusable. Although there are some technologies that are already implemented to minimize the effect of vibration, whether in the camera, like in-body image stabilization (IBIS), and the lens, like optical image stabilization (OIS), the effectiveness of those technologies to combat the vibration during the aerial mapping are unknown. Therefore, the best way to minimize the negative effect of the vibration is by utilizing the damping system, where the camera and the lens are attached to it.

It is necessary to know the vibration profile that affects the camera bay where the damping system is positioned in order to design an appropriate damping system. With the help of the Low-Cost Vibration and Impact Measurement System (LCVIMS) and covered in depth in this paper, the vibration profile should be recorded during the flight. Prior to integrating that system into the UAV, we should verify that it is operational and satisfies the performance specifications that will be discussed later in this chapter. As a result, we perform some vibration testing in a laboratory and then analyze the results. In order to conduct the vibration testing, a shaker must generate a certain pattern of vibration at a specific axis. The vibration generated by the shaker is then measured by two separate systems. The first system is a calibrated system named Medallion II VR9500. This system will validate the measurements of the second system, the LCVIMS, by contrasting the measurement result in both the frequency and time domains.

The Fast Fourier transform (FFT) method is used to change the measurement result in the time domain to the

frequency domain so we can understand what is causing the vibration. The frequency of the vibration source is one of the parameters that shape the vibration profile. In the time domain, the analysis will output two types of amplitude, which are the maximum amplitude, A_{max} , and the root mean square (RMS) of acceleration, a_{rms} . The use of the RMS value will achieve a smoother representation than using the clean vibration average because the clean vibration average is equal to zero¹⁹⁾. The calculation of the RMS value is using the following formula²⁰⁾, where N is the number of data obtained from the measurements and a_i is the acceleration in g unit.

$$a_{rms} = \sqrt{\frac{1}{N} \sum_{i=1}^N a_i^2} \tag{1}$$

The frequency, the A_{max} , and the a_{rms} are three parameters that shape the vibration profile. The LCVIMS should measure the vibration profile with good accuracy and precision. To validate the LCVIMS measurement, we compare the result with a professional and calibrated vibration measurement system, called as Medallion II VR9500. This system is equipped with the SENZ type 3055B2, an industrial-grade sensor. Based on the calibration report, this system is able to conduct a vibration measurement with maximum 2.0 % uncertainty between 20 to 2000 Hz frequency range. Therefore, this system is used as a reference system and the accuracy of the LCVIMS can be calculated by finding the differences in measurement between the LCVIMS with reference system. The calculation of difference is expressed in the percentage error values I as shown in the following equation, where the x_{LC} is the measurement result of the LCVIMS and the x_{MDL} is the measurement result of the Medallion II.

$$e = \frac{|x_{LC} - x_{MDL}|}{x_{MDL}} \times 100\% \tag{2}$$

By measuring the greatest amplitude’s divergence from the desired value, the precision of the LCVIMS is determined. Only the Z-axis is used to quantify precision in this study. The boxplot will be used to demonstrate the accuracy and precision of the LCVIMS in order to ensure a more explicit depiction. The performance requirements of the LCVIMS are described in terms of accuracy and precision, as shown in Table 2.

Table 2. Performance Requirement

No	Aspect	Requirement	Mean of Compliance
II.1	Accuracy of vibration measurement	The error of frequency, A_{max} , and a_{rms} measurement should be less than 15% across the tested frequency range and amplitude.	In the Vibration laboratory, the shaker will generate vibrations at the X, Y, and Z-axes with frequencies of 20, 40, 100, and 300 Hz and amplitudes of 1, 3, and 5 g. To effectively represent the measurement results, a bar chart should be used.
II.2	Precision of vibration	The amplitude deviation should be less than 15% across the tested frequency	In the Vibration laboratory, the shaker will generate vibrations at the Z-axes with frequencies of 20, 40, and 100 Hz and amplitudes of 1,

	measurement	range and amplitude.	3, and 5 g. To effectively represent the measurement results, a boxplot should be used.
II.3	Impact measurement	The error of peak value of impact measurement should be less than 5% at the tested case.	In the Vibration laboratory, the shaker will generate impact at the Z-axes with amplitudes of 5, 10, and 14 g. The impact frequency range is around 60 Hz, so the sampling rate 1024 Hz is sufficient to capture it.
II.4	In flight measurement	During the flight test, the LCVIMS should be able to record the vibration in the UAV camera bay.	The UAV will fly at a certain flight profile in a full flight phase (takeoff, climb, cruise, and landing). The LCVIMS should record the vibration, and the result should be presented in the time domain, using the amplitude of the acceleration (in g) vs. time (s) chart.

3. Design of Vibration and Impact Measurement System

This chapter discusses how we design the hardware of LCVIMS in order to fulfill the functionality requirement stated in Table 1. The discussion in this paper begins with the component selection. After we decide on the components that we will use, we will explain the general configuration of the LCVIMS and verify the final prototype fulfills the price, dimension, and weight requirements.

The component selection focuses on the selection of the microcontroller and the sensor that will be used by the LCVIMS. The microcontroller and the sensor are sorted out by analyzing the technical specification issued by the manufacturer. To simplify the development process, we use the microcontroller development board, which are printed circuit boards with a microcontroller/microprocessor mounted on them with some features and I/O capability. We are narrowing down the selection of the development board by applying two mandatory requirements, which are:

(1) The development board should be able to be programmed under Arduino IDE to accelerate the development process because we are familiar with the Arduino IDE and,

(2) According to requirement number I.3 and I.4, the development board should have a native SD/micro-SD card reader to minimize the risk of data logging failure during the test.

After doing some research online, we discovered not many options that fulfill the mandatory requirement. There are only three products available that fulfill those requirements, which are: (1) PJRC Teensy 4.1, (2) Freertronics EtherMega, and (3) Freertronics EtherTen. We will then compare the technical specification and choose one of the three contenders with the best technical specifications. During the comparison, we focus on the technical specification related to the fulfillment of the requirement, such as (1) The dimension, (2) the price, (3) The I/O capability, and (4) the processor speed. We use a simple scoring mechanism, where the first position gets 3 points and 1 point for the last position, as seen in Table 3.

Table 3. Selection and Scoring of Development Board

Parameter	Specification			Scoring			Remark
	(1)	(2)	(3)	(1)	(2)	(3)	
The Dimension (L X W) [cm]	6 X 1.8	12.5 X 9.5	7.1 X 5.3	3	1	2	The PJRC Teensy 4.1 has the smallest footprint between those three
The Price [\$]	31.50	48.82	44.13	3	1	2	The prices are taken from the website, without additional and shipping cost.
The I/O capability	I2C/SPI, Analog, Digital			3			All three candidates have the mandatory I/O to handle the communication with the sensor
The Processor	ARM Cortex-M7 at 600 MHz	Atmel ATmega328P at 16 MHz	Atmel ATmega2560 at 16 MHz	3	2	2	As mentioned in requirement I.3, higher processor speed is preferable.

Total Score	12	7	9	Based on this scoring, the Teensy 4.1 development board is selected.
--------------------	-----------	---	---	--

(1) PJRC Teensy 4.1, (2) Freetronics EtherMega, (3) Freetronics EtherTen

As mentioned in Table 1, the sensor is an accelerometer that should be small, thin, and lightweight to fulfill Requirement I.1. Therefore, we select the MEMS type of accelerometer, which is not only small, thin, and lightweight but also cost-effective, highly available, and commonly used for vibration measurement²¹). The performance of the MEMS accelerometer should fulfill Requirement I.3 in terms of frequency range and amplitude. The highest frequency that we want to measure is 400 Hz. Therefore, MEMS accelerometer should have a sampling rate of 1024 Hz, which is 2.56 times greater than the highest frequency of interest. The Sampling at a rate higher than 2.56 times the maximum frequency will ensure enough data is collected to reproduce the original signal. The maximum amplitude that we want to measure is 16g. Hence, the MEMS accelerometer should have a measurement range of -16 to +16g. After searching online through the internet, two strong candidates fulfill the requirements, which are: (1) Analog Device ADXL 345 and (2) InvenSense MPU-6050. Both candidates are able

to communicate with the Teensy 4.1 development board through the I2C or SPI interface using the highest possible data rate and have a similar price. However, the ADXL 345 has an advantage on the maximum sampling rate up to 3200 Hz over 1000 Hz on the MPU-6050. Hence, we select the ADXL 345 over the MPU-6050 because the ADXL345 has a higher maximum sampling rate that ensures better flexibility for future use. With the 3200 Hz sampling rate, the maximum frequency that we can measure is increasing to 1250 Hz.

Figure 2 shows the general configuration of the LCVIMS. There are two LED indicators, red and green, where the red LED indicates the system is ready to operate or in standby mode, while the green LED indicates the system is currently recording data. There is a push button to send a signal to the Teensy board to initiate the data recording process. The last component is the MicroSD Card, which serves as the storage medium for the recorded data. The SD card used in this system has a capacity of 32 Gb and a minimum class rating of 10.

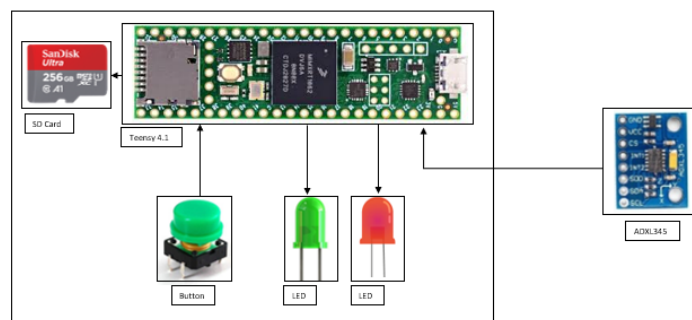


Fig. 2: General Configuration of the LCVIMS

The cost estimation to build the LCVIMS is shown in Table 4. The price listed in the table is the original price from the website, without additional and shipping cost. As shown Table 4, the total budget required to build one system is approximately USD 62.84. Therefore, with a cost less than 100 USD, the LCVIMS are considered as

cost-effective solution. The comparable commercial product that available in the market will be Siemens Scadas XS. However, the price of that instrument will be much higher compared to our solution. Currently, there is no similar system in the market that have the same price point with our system.

Table 4. Calculation of Cost for LCVIMS

Part	Price (USD)	Qty	Total Price (USD)
PJRC Teensy 4.1	31.50	1	31.50
SparkFun Triple Axis Accelerometer Breakout - ADXL345	20.50	1	20.50

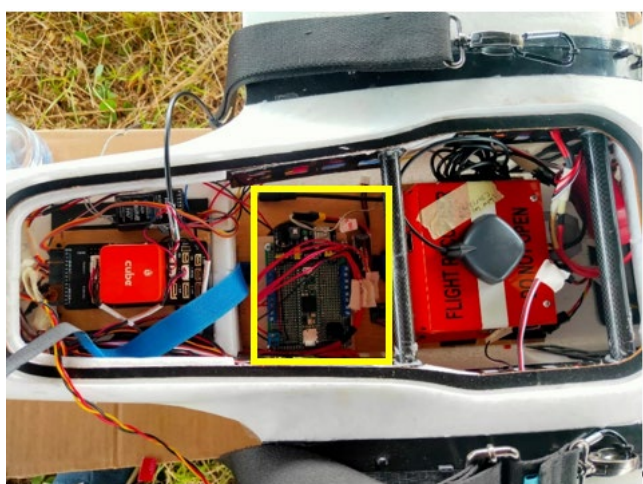
Power Supply Module	0.78	1	0.78
Push button	0.10	1	0.10
LED	0.01	2	0.02
Prototype PCB	0.43	1	0.43
Cable	0.10	3	0.30
Terminal Block Screw	0.092	10	0.92
Tattu 450mAh 7.6V High Voltage 95C 2S1P Lipo Battery Pack	8.29	1	8.29
Total Price			62.84

The total weight of the LCVIMS is less than 120 grams, as shown in Fig. 3(a), including the DC power supply. In this case, we use the LiPO battery. The dimension of the

LCVIMS is fitted into the UAV cabin bay, as shown in Fig. 3(b). Both weight and dimension fulfill Requirement I.1.



(a)



(b)

Fig. 3: (a) the Total Weight of the LCVIMS. (b) The LCVIMS (Yellow Rectangle) Installed on the UAV

The LCVIMS is built using firmware developed using the Arduino IDE with the C language. The Arduino Integrated Development Environment is an application that runs on multiple platforms and is built with functions from C and C++. It is used to write and upload programs to Arduino-compatible boards, as well as other vendor development boards with the help of third-party cores²³. The open-source Arduino Software (IDE) simplifies the process of writing code and uploading it to the

development board, and it can be used with any Arduino board. The simplified programming flowchart is shown in Fig. 4. The vibration measurements obtained from this device are stored on an SD card. It is difficult to obtain high sampling rates when using SD cards for data storage²⁴. However, by using the SdFat interface library developed by Greiman, a sufficient sampling rate can be achieved for vibration measurements.

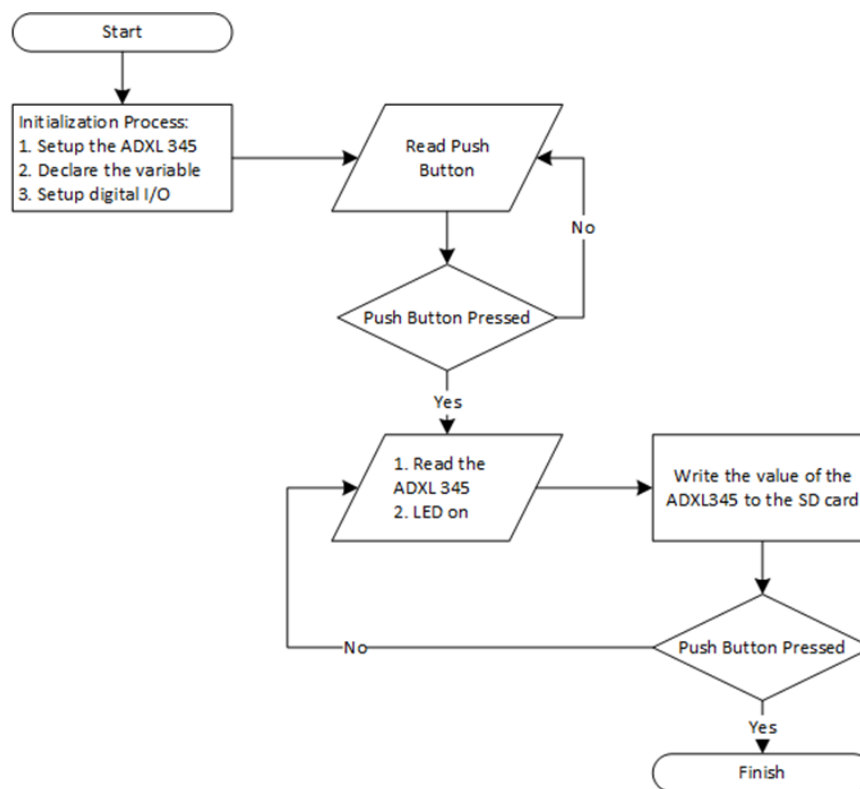


Fig. 4: The simplified flowchart of the firmware design

4. Experimental Setup

In this chapter, we explain in detail the ground and flight test setup of the LCVIMS. We carried out the test in order to verify and validate the performance of the LCVIMS against the performance requirement, as stated in Table 2.

4.1 Ground Test Setup

As explained in Chapter 2, the validation of LCVIMS is carried out by comparing the results of the LCVIMS with a professional system. The professional system used in the validation activities is the Medallion II VR9500 manufactured by Vibration Research. The Medallion II VR9500 is a vibration control module with a 4-channel vibration measurement system. The main function of the Medallion II VR9500 is to command and control the shaker to shake and vibrate at certain patterns, such as swept and/or fixed-frequency sine wave tests with control of acceleration, velocity, and displacement. The shaker used in the test is the type 4809 manufactured by B&K. The shaker needs an amplified signal from the Medallion II VR9500. Therefore, the type 2706 amplifier manufactured by B&K is used to amplify the signal. To measure the vibration from the shaker, an industrial-grade accelerometer from SENZ type 3055B2 is connected to

the Medallion II VR9500. During the ground test, a rigid aluminum plate was installed on the top of the shaker. Then, the SENZ type 3055B2 was mounted on the aluminum plate to sense the vibration of the shaker. The accelerometer from the LCVIMS was mounted on the same aluminum plate as well. However, to simplify the installation of the LCVIMS accelerometer during the X and Y-axis vibration testing, we added a rigid block of aluminum. Figure 5 shows the sensor placement during the vibration test for the X, Y, and Z-axis, while Fig. 6 shows the complete schematic of the vibration and impact test.

The execution of the ground test is started with the identification of the maximum sampling rate that can be achieved by the LCVIMS. The procedure for this test is varying communication protocol (I2C/SPI) between the development board and the sensor as well as the number of axes or sensors used at once. After finding the best configuration that has the fastest sampling rate, the ground testing was performed according to Table 2. The data obtained from the test results were processed using MATLAB computing programming²⁵. The vibration data were analyzed in both the time domain and frequency domain.

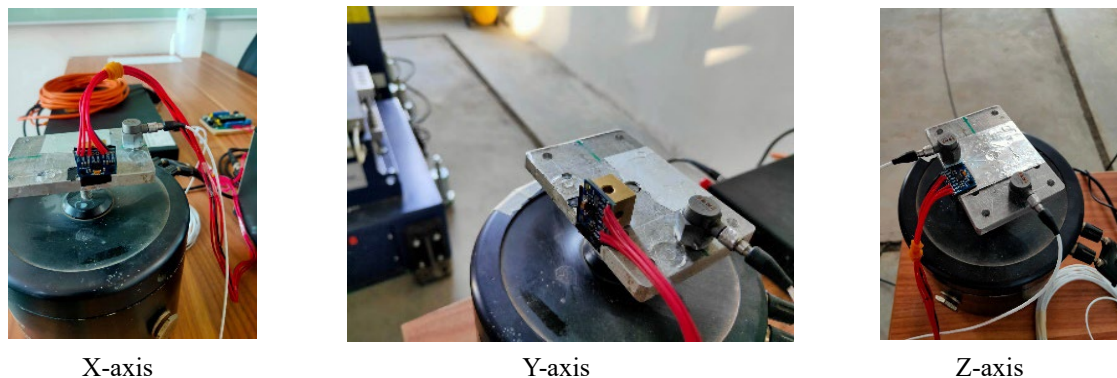


Fig. 5: Set-Up of Sensor on the Shaker for Vibration Test

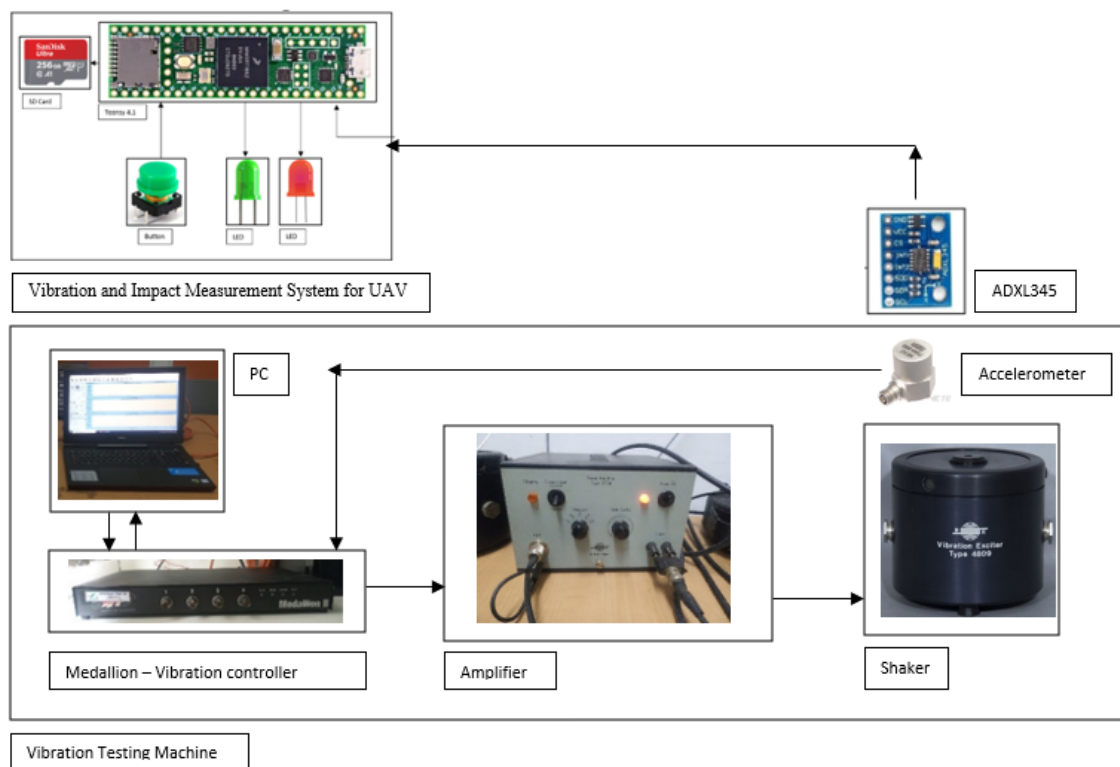


Fig. 6: The Schematic of Impact and Vibration Test

4.2 Flight Test Setup

For the flight test, we used the UAV frequently used for aerial mapping. This UAV was chosen because it has good flight endurance, allowing it to cover large areas in a single flight during aerial mapping²⁶. However, since this UAV is a commercial product, there is no information about the vibration profile, especially at the camera bay during the

flight. Hence, as explained in Chapter 2, the purpose of flight tests is to determine the vibration characteristics that occur in the camera location under actual conditions²⁷. This is important because these vibrations significantly impact the results of photography with this aircraft. Furthermore, this research will be useful for designing a vibration-damping device for the camera position.



Fig. 7: (a) Payload and Instrumentation Setup Before Flight (b) Take-off launch

4.2.1 UAV Specification

The UAV has a conventional configuration, a twin-engine, and a nearly rectangular wing. This aircraft can fly over 3 hours and cover approximately 180 km with two batteries, specifically 22.2V 15C 6S 16000mAh. The aircraft is also made of EPO Foam and reinforced with a carbon frame in the wings and horizontal and vertical tails.

Since the aircraft is lightweight and does not have landing gear, the takeoff method involves hand-launching. Like other unmanned aircraft, this aircraft is controlled using a remote control operated by a pilot to carry out the aerial photography mission. The detailed specification of the MFE Fighter aircraft is provided in Table 5.

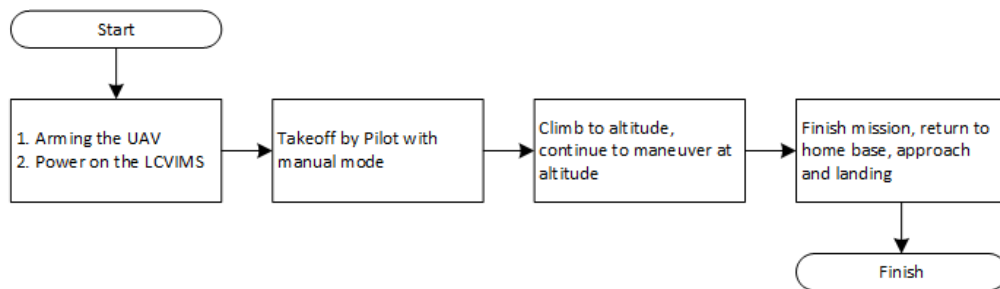


Fig. 8: Flight test plan for testing the LCVIMS

Table 5. Specification of MFE Fighter aircraft

Parameters	Value	Type/Unit
Fuselage length	1.41	m
Wing Span	2.43	m
Wing Area	0.725	m ²
Payload Weight	2	kg
MTOW	10	kg
Engine	Electric, 2 X 3520 KV500 Motor	
Battery	2 X LiPo 6S 16.000 mAh	
Telemetry range	Line of Sight (LOS) 10 Km – tested	
RC receiver	Futaba S-Bus 2 Km	

Take-off Method	Hand throw launch
Landing Method	Belly landing
Material	EPO Foam, EVA Foam, Carbon Fiber (Spar)

4.2.2 Flight Test Plan

Before the pilot flies the aircraft, the flight profile is determined. The data acquisition equipment is tested to determine the vibration characteristics during takeoff, pilot-controlled maneuvers, and landing²⁸⁾. This is conducted because, during takeoff, the pilot provides throttle input ranging from 75% to 100%, which increases the engine RPM and causes vibrations in the aircraft, especially in the camera location. After reaching an altitude of 200 meters, the pilot provides control surface and throttle input through the RC system, causing the aircraft to maneuver and experience speed changes. Once on cruise flight, the pilot controls the aircraft for landing. The flow diagram of the test and the vibration data acquisition during flight are provided in Fig. 8.

5. Results and Discussions

After obtaining the data with the testing setup mentioned in the previous section, a more in-depth

analysis was performed. There are two analyses that will be discussed in this section, namely the analysis of the Ground Test results and the analysis of the Flight Test results.

5.1 Ground Test Result Analysis

In the previous discussion, it has been explained that Ground Test is carried out by conducting vibration testing and impact testing.

5.1.1 Vibration Test Result

The measurement results of the LCVIMS compared to the Medallion are shown in Fig. 9, which illustrates how both systems measure vibrations in the X, Y, and Z directions for a 20 Hz input frequency with a 1 g input amplitude. Both systems can measure acceleration in all three axes with amplitudes that are very close with slight differences in frequency.

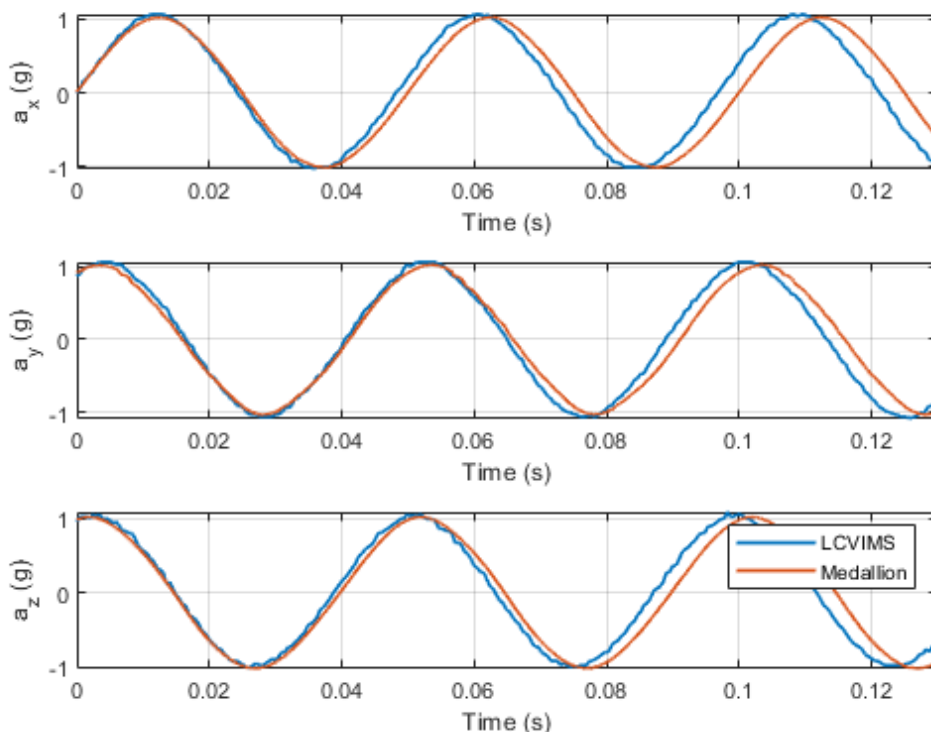


Fig. 9: Vibration Measurement Result of LCVIMS and Medallion in Three Axes

The calculation results in vibrational parameters are presented in the form of bar charts in Fig.10 until Fig.12. From these three figures, the percentage error of both systems is less than 15%. The percentage error for frequency measurements is even less than 6%. Meanwhile, for arms and Amax measurements, vibration measurements in the Z axis result in less than 10% percentage errors. These figures also show that LCVIM meets the accuracy requirement specified in Table 2 because all percentage errors are below 15%. It can even be seen in several cases that the percentage errors are close to 0%, such as the frequency error difference in the test with a frequency of 300 Hz and the arms error difference in the test on the z-axis with a frequency of 20, 40, and 100 Hz.

A more detailed analysis was performed on the amplitude Amax values in the z-direction to assess the level of accuracy and precision of LCVIMS. Therefore, a boxplot was used for the tests with amplitudes (A) of 1, 3, and 5g and frequencies of 20, 40, and 100 Hz, as shown in Fig. 13. These boxplot graphs show that the amplitude test data results of Medallion have a box that tends to be symmetrical, whereas some LCVIMS test results are

skewed. The symmetrical box shows that the data follow a normal distribution, so the mean equals the median. The amplitude deviation can be analyzed from the length of the box, which is the interquartile range (IQR). The IQR values of the Medallion data are much narrower than the LCVIMS data. It means that Medallion, as a validator, resulted in more consistent measurement results. The IQR values of LCVIMS amplitude data are relatively small, as shown by the boxes that are not too long. The longest box is found in the test case with a frequency of 100 Hz and an amplitude of 5g, but this value still meets the performance requirement for precision shown in Table 2. Hence, LCVIMS is proven to be precise.

In terms of accuracy, the median value between LCVIMS and Medallion is quite close. It shows that the accuracy of LCVIMS is sufficient to meet the requirement. In addition, from these boxplot graphs, we conclude that in the range of amplitudes and frequencies tested, the increase in amplitude and frequency values does not affect the accuracy of LCVIMS. However, the higher the measured vibration amplitude, the level of precision tends to decrease, especially in the case with a frequency of 100 Hz and an amplitude of 5g.

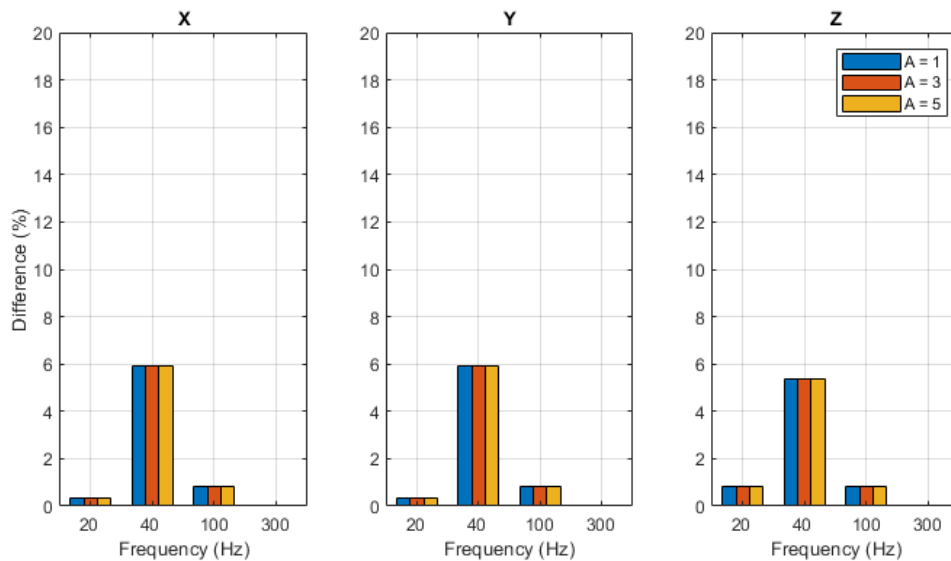


Fig. 10: The LCVIMS Frequency Error Difference Compared to Validator

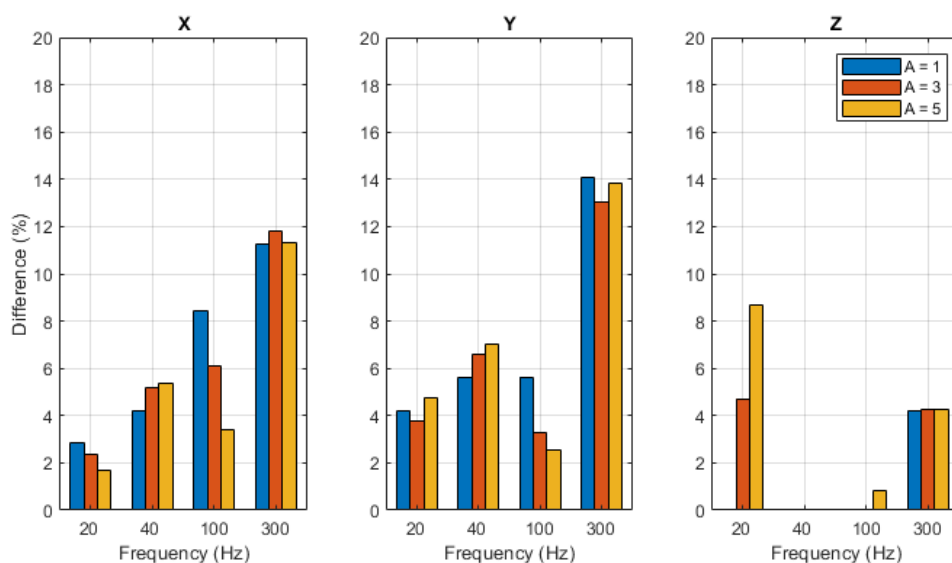


Fig. 11: The LCVIMS a_{rms} Error Difference Compared to Validator

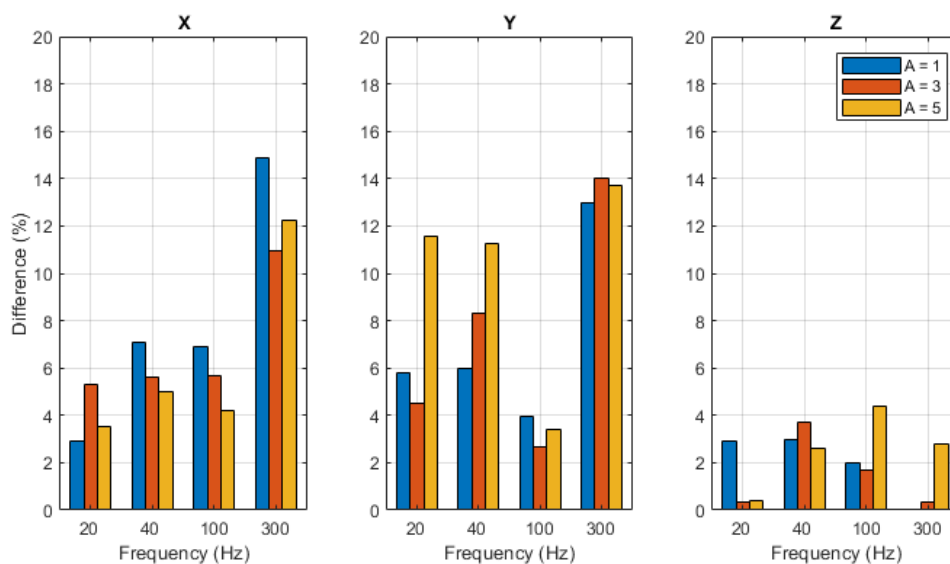


Fig. 12: The LCVIMS A_{max} Error Difference compared to the validator

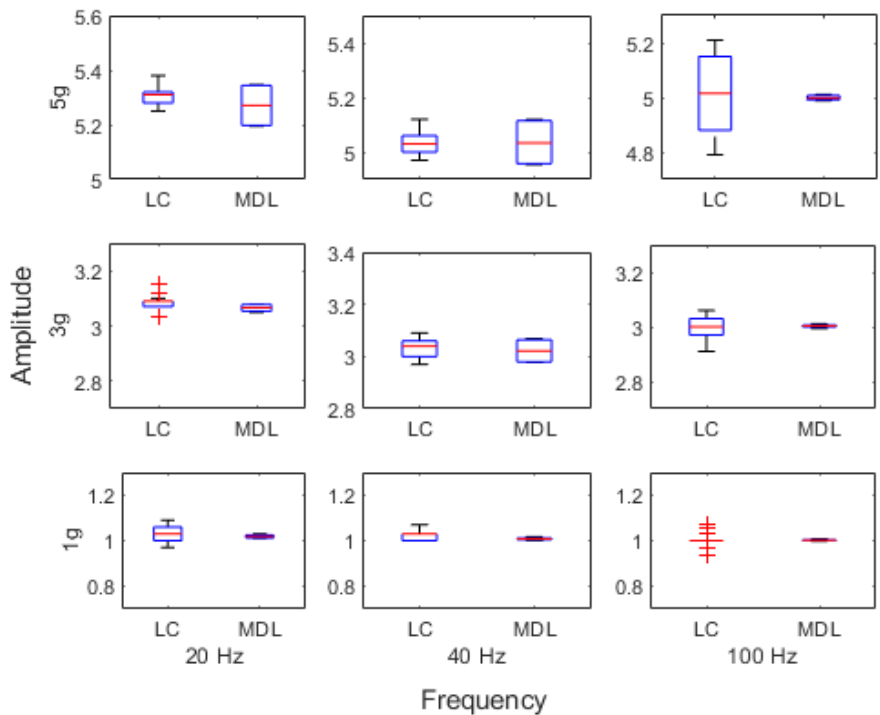


Fig. 13: Boxplot Graphs of Amplitude A_{max} in z-Direction

5.1.2 Impact Test Result

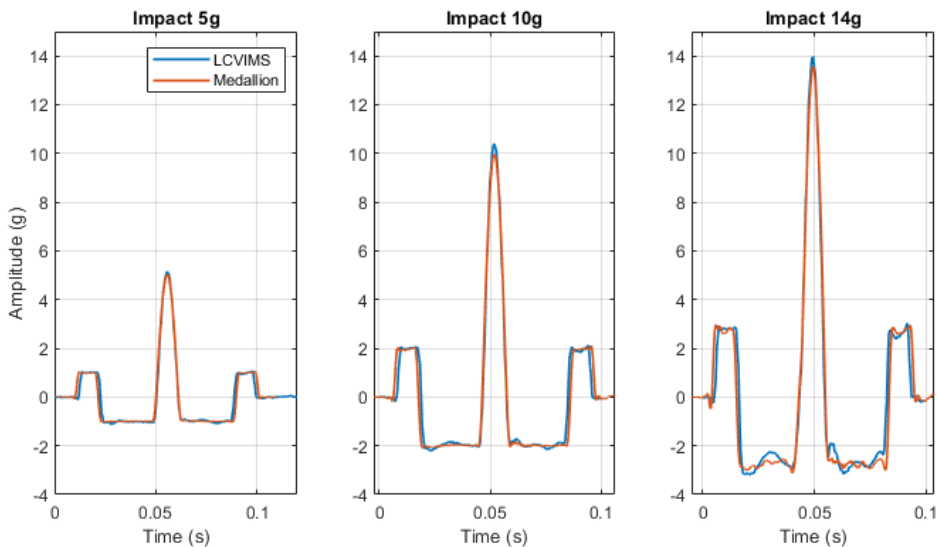


Fig. 14: Impact Test Result Comparison of LCVIMS and Medallion

The impact test results for both modules can be seen in Fig. 14. From this figure, the test data shows quite similar results between LCVIMS and Medallion for each case. At a 5g impact load, the measurement difference is only 2%. Then, at the 10G impact load, the measurement difference is approximately 4%, where the LCVIMS result is slightly above the Medallion result at the peak value. Meanwhile, at 14G impact load, the measurement reading difference is less than 3%. The measurement results indicate that the developed LCVIMS can read impact loads close to the Medallion, and it meets the requirement mentioned in

Table 2 for impact measurement. Therefore, this LCVIMS can generally measure impact loads on UAV aircraft.

5.2 Flight Test Result Analysis

As stated in the requirement, this LCVIMS must be proven to record vibration data during flight. Therefore, a flight test, as explained in the previous section, was conducted. The recorded data in the time domain are shown in Fig. 15.

The flight test was carried out with a simple mission of

16.66 minutes. During the flight, LCVIMS could measure the acceleration of $-9.03 - 11.28g$. Generally, this vibration measurement result can be divided into 3 phases: take-off-climb, cruise, and descent-impact-landing. We conduct the preflight check and the initialization of the LCVIMS on ground for 600 s prior to the flight test. We keep the data because we want to show that the LCVIMS is working and recording the data during that period.

It is shown in Fig. 15 that during the take-off-climb phase, the UAV speed was increased significantly so that the engine RPM increased. This increase in engine RPM resulted in a higher vibration. It also happened during the cruise phase. The sampling rate specification on the LCVIMS is 1024 Hz, which means ± 1 sample per 1 ms. Meanwhile, the impact measured on the landing phase with a peak of 11.28 G has a period of ± 29 ms (as seen in the sub figure "Landing Impact"). This means the sampling rate on the LCVIMS is more than sufficient to capture the impact that occurs. An FFT analysis was carried out in the range of the take-off-climb phase to the cruise (600 – 860 s) to observe the frequency that occurred on the UAV. The result of the FFT analysis is shown in Fig. 16. In the 10 – 100 Hz frequency range, there are 4 dominant frequencies, namely 15.43, 24.1, 48.64, and 72.43 Hz.

This flight test result concludes that the LCVIMS can record UAV vibration and impact phenomena.

6. Conclusions and future works

In this research, the development of the LCVIMS system applicable to UAVs has been successfully accomplished. A series of processes were carried out, starting from design and requirement determination, Vibration and Impact Measurement system design process, ground tests including vibration and impact tests, and finally, flight tests on the unmanned MFE Fighter aircraft in real flight conditions. The LCVIMS design yielded satisfactory results compared to existing products on the market. However, upgrading the accelerometer specifications is recommended to improve the performance of the LCVIMS so it can capture at least 5 sample point of the wave profile.

Cost analysis conducted on the developed system indicates that the total component cost does not exceed USD 100; more precisely, the total cost amounts to USD 62.84. The designed system also meets both functional and performance requirements. A comparison of vibration test results at a frequency of 20 Hz and an amplitude of 1 G shows differences in measurement results with the commercial module "Medallion" in the range of 10%, with some parameters even below 6%. The impact test results also demonstrate excellent measurement differences of 2-4%. Flight tests also indicate that the LCVIMS system can accurately record vibration and impact phenomena according to the executed flight missions.

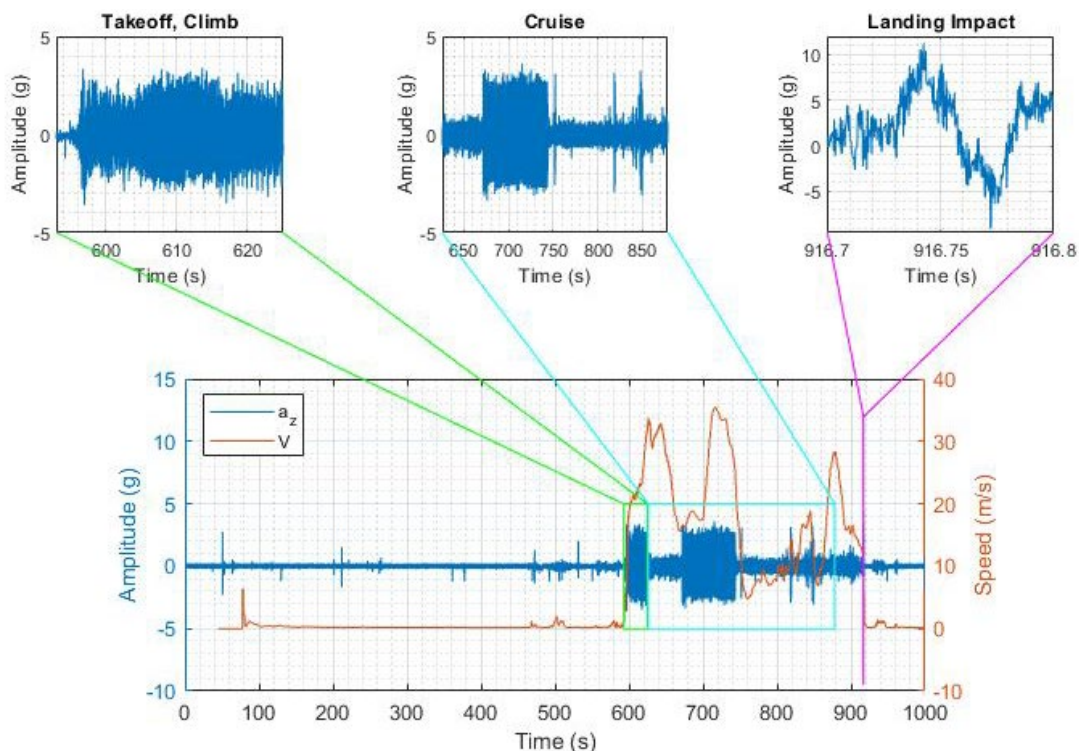


Fig. 15: Flight Test Data Recorded

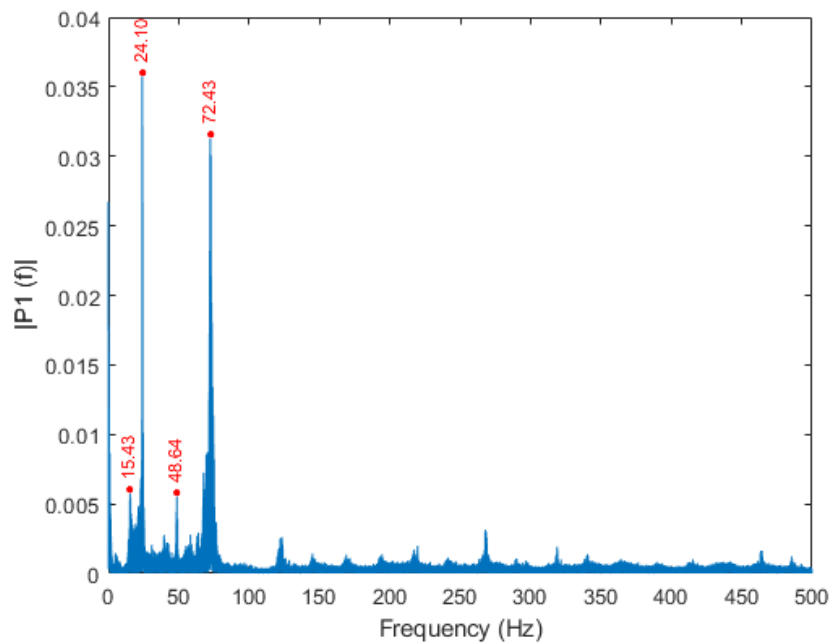


Fig. 16: FFT Result in Range of 600 – 860 s

Further research can be conducted to refine the LCVIMS system. Environmental tests to assess the effect of temperature on the system's performance should be carried out to enhance its reliability. Design for manufacture and assembly analysis should also be performed to accurately calculate the system's costs. Additionally, flight tests on other UAV variants should be conducted to make the LCVIMS module design more robust LCVIMS system. Environmental tests to assess the effect of temperature on the system's performance should be carried out to enhance its reliability. Design for manufacture and assembly analysis should also be performed to accurately calculate the system's costs. Additionally, flight tests on other UAV variants should be conducted to make the LCVIMS module design more robust. At the later stage, we will use the data from the LCVIMS to develop the structural health monitoring that will alert the UAV operator if there any possibilities of structural crack.

Acknowledgements

This work is supported by the project of “Development of a vibration characteristic identification system for UAV during flight” No.6/III/HK/2022. We also acknowledge the support from project “Drone Precision Mapping” No 3/III.1/HK/2023. Both are under the grant of Research Organization for Aeronautics and Space of National Research and Innovation Agency (BRIN), Bogor, Indonesia.

Nomenclatures

a_{rms}	Root mean square value of acceleration (g)
a_z	Acceleration in Z-axis (g)
A_{max}	Amplitude (g)
DC	Direct Current
e	Percentage error value (%)
FFT	Fast Fourier Transform
GLRT	Generalized Likelihood Ratio Test
IBIS	In-body image stabilization
LCVIMS/LC	The low-cost vibration and impact measurement system
MDL	Medallion
N	Number of data (-)
OIS	Optical image stabilization
PI	FFT Magnitude (-)
PSO	Particle Swarm Optimization
SVM	Support Vector Machine
UAV	Unmanned Aerial Vehicle
V	Airspeed of the aircraft (m/s)

References

- 1) M. Abdulrahman Al-Mashhadani, “Random vibrations in unmanned aerial vehicles, mathematical analysis and control methodology based on expectation and probability,” *Journal of Low Frequency Noise, Vibration and Active Control*, **38**

- (1) 143–153 (2019). doi: 10.1177/1461348418813031.
- 2) L.N. Patil, H.P. Khairnar, J.A. Hole, D.M. Mate, A. V. Dube, R.N. Panchal, and V.B. Hiwase, “An experimental investigation of wear particles emission and noise level from smart braking system,” *Evergreen*, **9** (3) 711–720 (2022). <https://doi.org/10.5109/4843103>.
 - 3) H. Jiang, S. Li, J. Li, Y. Su, Z. Li, and J. Liu, “Effect of vibration on the aerodynamic behavior of a 5:1 rectangular cylinder,” *Journal of Wind Engineering and Industrial Aerodynamics*, **225** 104995 (2022). doi: 10.1016/j.jweia.2022.104995.
 - 4) R. Li, M. Karma, and C. Hu, “Two-dimensional viv simulation of a cylinder close to a wall with high reynolds number by overset mesh,” **10** (01) 219–229 (2023). doi: -
 - 5) M. Kumar and M. Devendra, “Characterisation of road vibration environment for a UAV transport container,” in 2017 International Conference on Nascent Technologies in Engineering (ICNTE), Jan. 2017, pp. 1–6. doi: 10.1109/ICNTE.2017.7947902.
 - 6) S. Radkowski and P. Szulim, “Analysis of vibration of rotors in unmanned aircraft,” in 19th International Conference on Methods and Models in Automation and Robotics (MMAR), 748–753 (2014). doi: 10.1109/MMAR.2014.6957449.
 - 7) E. Fresk and G. Nikolakopoulos, “Frame induced vibration estimation and attenuation scheme on a multirotor helicopter,” in 53rd IEEE Conference on Decision and Control, 5698–5703 (2014). doi: 10.1109/CDC.2014.7040281.
 - 8) G. Cai, L. Feng, B. M. Chen, and T. H. Lee, “Systematic design methodology and construction of UAV helicopters,” *Mechatronics*, **18** (10), 545–558, (2008). doi: 10.1016/j.mechatronics.2008.05.011.
 - 9) M. Dunbabin, S. Brosnan, J. Roberts, and P. Corke, “Vibration isolation for autonomous helicopter flight,” in IEEE International Conference on Robotics and Automation, **4** 3609–3615 (2004). doi: 10.1109/ROBOT.2004.1308812.
 - 10) G. N. M. Plasencia, M. T. Rodríguez, S. C. Rivera, and Á. H. López, “Modelling and Analysis of Vibrations in a UAV Helicopter with a Vision System,” *International Journal of Advanced Robotic Systems*, **9** (5) 220 (2012). doi: 10.5772/52761.
 - 11) W. Luber and J. Becker, “Application of PVDF foils for the measurements of unsteady pressures on wind tunnel models for the prediction of aircraft vibrations,” *Structural Dynamics*, **3** 1157–1176 (2011). doi: 10.1007/978-1-4419-9834-7_102.
 - 12) Y.-C. Lai and S.-S. Jan, “Attitude estimation based on fusion of gyroscopes and single antenna GPS for small UAVs under the influence of vibration,” *GPS Solutions*, **15** (1) 67–77 (2011). doi: 10.1007/s10291-010-0171-y.
 - 13) J. Simsiriwong and R. W. Sullivan, “Experimental Vibration Analysis of a Composite UAV Wing,” *Mechanics of Advanced Materials and Structures*, **19** (1–3) 196–206 (2012). doi: 10.1080/15376494.2011.572248.
 - 14) A. Nemra and N. Aouf, “Robust INS/GPS Sensor Fusion for UAV Localization Using SDRE Nonlinear Filtering,” *IEEE Sensors Journal*, **10** (4) 789–798 (2010). doi: 10.1109/JSEN.2009.2034730.
 - 15) S. Urbano, E. Chaumette, P. Goupil, and J.-Y. Tourneret, “Aircraft Vibration Detection and Diagnosis for Predictive Maintenance using a GLR Test,” *IFAC-PapersOnLine*, **51** (24) 1030–1036 (2018). doi: 10.1016/j.ifacol.2018.09.716.
 - 16) Zhang Jianjun, Li Ming, Sun Jianyong, and Chang Haijuan, “Prediction of aircraft vibration environment based on support vector machines with particle swarm optimization algorithm,” in International Conference on Automatic Control and Artificial Intelligence, 1592–1595 (2012). doi: 10.1049/cp.2012.1288.
 - 17) C. Robbe, A. Papy, and N. Nsiampa, “Using kinetic energy non-lethal weapons to neutralize low small slowunmanned aerial vehicles,” *Human Factors and Mechanical Engineering for Defense and Safety*, **2** 1 (2018). doi:10.1007/s41314-018-0008-y.
 - 18) B. Hunter, A.A. Swidan, K. Joiner, and G. Hazenberg, “Accurate prediction of landing loads for a new design of a wing-in-ground maritime surveillance drone - cfd investigation,” 31st International Conference on Computer Theory and Applications, 11–17 (2021). doi: 10.1109/ICCTA54562.2021.9916598.
 - 19) A. Quagliata, M. Ahearn, E. Boeker, C. Roof, L. Meister, and H. Singleton. “Transit Noise and Vibration Impact Analysis Manual”. FTA Report No. 0123. Massachusetts, United States (2018).
 - 20) P.J. Rzeszucinski, J.K. Sinha, R. Edwards, A. Starr, B. Allen, “Normalised Root Mean Square and Amplitude of Sidebands of Vibration Response as Tools for Gearbox Diagnosis,” *Strain*, **48** (6) 445–452 (2008). doi: 10.1111/j.1475-1305.2012.00839.x.
 - 21) R.R. Ribeiro, and R. de M. Lameiras, “Evaluation of low-cost mems accelerometers for shm: frequency and damping identification of civil structures,” *Latin American Journal of Solids and Structures*, **16** (7) e203 (2019). doi:10.1590/1679-78255308.
 - 22) S. Komarizadehasl, B. Mobaraki, H. Ma, J.A. Lozano-Galant, J. Turmo, “Development of a Low-Cost System for the Accurate Measurement of Structural Vibrations,” *Sensors*, **21** (18) 6191 (2021). doi: 10.3390/s21186191
 - 23) T. Sulistyono, K. Achmad, and I.B.I. Purnama, “Empowering low-cost survey instrument for the stake-out measurements using android application,” *Evergreen*, **8** (3) 610–617 (2021). <https://doi.org/10.5109/4491653>.
 - 24) A. González, J.L. Olazagoitia, and J. Vinolas, “A low-

cost data acquisition system for automobile dynamics applications,” *Sensors*, **18** (2) 366 (2018). doi: 10.3390/s18020366.

- 25) N. Kumari, S.K. Singh, and S. Kumar, “MATLAB-based simulation analysis of the partial shading at different locations on series-parallel pv array configuration,” *Evergreen*, **9** (4) 1126–1139 (2022). <https://doi.org/10.5109/6625724>
- 26) D.D.D.P. Tjahjana, I. Yaningsih, B.Y.L. Imama, and A.R. Prabowo, “Aerodynamic performance enhancement of wing body micro uav employing blended winglet configuration,” *Evergreen*, **8** (4) 799–811 (2021). <https://doi.org/10.5109/4742122>.
- 27) G. Burshukova, A. Kanazhanov, R. Abuova, and A. Joldassov, “Analysis of using damping alloys to improve vibration and strength characteristics in the automotive industry,” *Evergreen*, **10** (2) 742–751 (2023). <https://doi.org/10.5109/6792824>.
- 28) I.T. Setyadewi, and P.S. Priambodo, “Study and analysis of crosstalk reduction in uav cabling by using various cable types,” *Evergreen*, **9** (1) 150–155 (2022). <https://doi.org/10.5109/4774232>.